THE JOURNAL OF BIOLOGICAL CHEMISTRY VOL. 291, NO. 44, pp. 22924–22935, October 28, 2016
Published in the U.S.A.

Structural Diversity in the Type IV Pili of Multidrug-resistant *Acinetobacter*[*][S]

Received for publication, August 1, 2016, and in revised form, September 7, 2016 Published, JBC Papers in Press, September 15, 2016, DOI 10.1074/jbc.M116.751099

Kurt H. Piepenbrink[‡1], Erik Lillehoj[§], Christian M. Harding[¶], Jason W. Labonte[‖2], Xiaotong Zuo[‖], Chelsea A. Rapp[‡], Robert S. Munson, Jr.[**], Simeon E. Goldblum[‡‡§§¶¶], Mario F. Feldman[¶], Jeffrey J. Gray[‖], and Eric J. Sundberg[‡ ‡‡‖‖3]

From the [‡]Institute of Human Virology and Departments of [‡‡]Medicine, [‖‖]Microbiology and Immunology, [§]Pediatrics, and [¶¶]Pathology, University of Maryland School of Medicine, Baltimore, Maryland 21201, [§§]Baltimore Veterans Affairs Medical Center, Baltimore, Maryland 21201, [‖]Department of Chemical and Biomolecular Engineering, Whiting School of Engineering, The Johns Hopkins University, Baltimore, Maryland 21218, [**]The Center for Microbial Pathogenesis in the Research Institute at Nationwide Children's Hospital and Department of Pediatrics, The Ohio State University College of Medicine, Columbus, Ohio 43205, and [¶]Department of Molecular Microbiology, Washington University School of Medicine, St. Louis, Missouri 63110

***Acinetobacter baumannii* is a Gram-negative coccobacillus found primarily in hospital settings that has recently emerged as a source of hospital-acquired infections. *A. baumannii* expresses a variety of virulence factors, including type IV pili, bacterial extracellular appendages often essential for attachment to host cells. Here, we report the high resolution structures of the major pilin subunit, PilA, from three *Acinetobacter* strains, demonstrating that *A. baumannii* subsets produce morphologically distinct type IV pilin glycoproteins. We examine the consequences of this heterogeneity for protein folding and assembly as well as host-cell adhesion by *Acinetobacter*. Comparisons of genomic and structural data with pilin proteins from other species of soil gammaproteobacteria suggest that these structural differences stem from evolutionary pressure that has resulted in three distinct classes of type IVa pilins, each found in multiple species.**

Type IV pili are extracellular adhesive appendages primarily comprising a single protein subunit, called the major pilin, which is assembled into a narrow (~6–9-nm) helical fiber of variable length (up to 2.5 μm) (1). One or more other proteins, called minor pilins, are also incorporated into the fiber at low levels. All pilins contain an N-terminal signal sequence followed by an ~30-amino acid hydrophobic α-helix resembling a transmembrane domain (the α1-N domain). This is, in turn, followed by a soluble ~15-kDa globular domain referred to as the pilin headgroup; the hydrophobic helical regions are buried together in the center of the fiber, whereas portions of the C-terminal headgroup are exposed (2, 3).

Type IV pili are found in both Gram-negative (4, 5) and Gram-positive (6–8) bacteria as well as Archea (9). They are involved in a wide range of processes, including twitching motility (10), horizontal gene transfer (11), host-cell adhesion (12), and microcolony/biofilm formation (13). This functional diversity is reflected in the sequence of the pilin proteins that typically have little or no sequence identity beyond the hydrophobic portion of the N-terminal α-helix. This lack of sequence identity is apparent even in cases where there is high structural similarity.

In contrast, within a given species, the minor pilins are typically well conserved. Only the major pilin is highly variable (14–16) and then only in those regions left exposed in the assembled pilus (17). This sequence diversity may result from diversifying selection as a mechanism by which to avoid detection by the host immune system (18). However, such diversity can also be found in species whose life cycle is primarily environmental (19). Glycosylation is an additional source of variability in some type IV pilins; *O*-linked glycosylation has been observed in multiple strains of both *Pseudomonas aeruginosa* (20–22) and *Neisseria* (23, 24). Additional glycosylation sites have been found in class II strains of *Neisseria meningitidis* where they have been hypothesized to play a role in immune evasion (25).

Among the many genera of Gram-negative bacteria that express type IV pili is *Acinetobacter*, a coccobacillus that is widely distributed in nature and can be isolated from the environment in the soil and in water as well as from a variety of mammalian hosts (26, 27). Several species of *Acinetobacter*, chiefly *Acinetobacter baumannii*, *Acinetobacter calcoaceticus*, *Acinetobacter nosocomialis*, and *Acinetobacter pittii*, are collectively referred to as the *A. calcoaceticus-baumannii* (Acb)[4] complex and constitute an increasingly common source of nosocomial infections (28–30). Although reports of infections by *A. baumannii* predominate in the literature, phenotypic similarity makes it difficult to differentiate between related *Acineto-*

[*] This work was supported in part by National Institutes of Health Grant R01 AI114902 (to E. J. S.). The authors declare that they have no conflicts of interest with the contents of this article. The content is solely the responsibility of the authors and does not necessarily represent the official views of the National Institutes of Health.

[S] This article contains supplemental Figs. 1–6.

The atomic coordinates and structure factors (codes 4XA2, 5IHJ, and 5CFV) have been deposited in the Protein Data Bank (http://wwpdb.org/).

[1] Supported by National Institutes of Health Training Grant T32 AI095190 and National Institutes of Health Fellowship F32 AI110045.
[2] Supported by National Institutes of Health Fellowship F32 CA189246.

[3] To whom correspondence should be addressed. E-mail: esundberg@ihv.umaryland.edu.

[4] The abbreviations used are: Acb, *A. calcoaceticus-baumannii*; MBP, maltose-binding protein; Bis-Tris, 2-[bis(2-hydroxyethyl)amino]-2-(hydroxymethyl)propane-1,3-diol; MPD, 2-methyl-2,4-pentanediol; PAK, *P. aeruginosa* strain K; OTase, oligosaccharyltransferase; r.m.s.d., root mean square deviation.

bacter species (31), and in model organisms, all four species have been found to be infectious (32).

Like other *Acinetobacter* species, *A. baumannii* lacks flagella but exhibits twitching motility, which is dependent on type IV pili (33). Type IV pili are also required for its natural transformation (33, 34), but their role in other biological processes is unclear. Virstatin, a known inhibitor of type IV pilus formation in *Vibrio cholerae*, was shown to both reduce type IV pilus expression and inhibit biofilm formation in *A. baumannii* (35). In another study, no correlation could be demonstrated between antigenic variation in the *A. baumannii* major pilin, *pilA*, and biofilm formation *in vitro* (36). More recently, Oh and Choi (37) reported that deletion of a LuxR-type regulator, AnoR, reduces both biofilm formation and surface motility in *A. nosocomialis* ATCC 17903. In addition to variation in the sequence of *pilA*, some *Acinetobacter* strains utilize an *O*-oligosaccharyltransferase to specifically glycosylate the major pilin at a C-terminal serine with the major capsule polysaccharide repeat unit (38, 39). These post-translational modifications are independent of the more general protein *O*-glycosylation system common to many gammaproteobacteria (including *P. aeruginosa* and *Dichelobacter nodosus*) (40–43). However, Harding *et al.* (38) reported that pilin C-terminal glycosylation is not required for either competence or twitching motility.

To understand the basis for the variability in sequence and glycosylation of *Acinetobacter* PilA, we have resolved the x-ray crystal structures of the major type IV pilin from three members of the Acb complex, strains ACICU and BIDMC 57 of *A. baumannii* and strain M2 of *A. nosocomialis.* In these three structures, we observe structural divergence independent of species within *Acinetobacter*. We demonstrate that *Acinetobacter* type IV pili promote host-cell adhesion in a manner independent of C-terminal glycosylation. We also provide evidence that the structural variation of *Acinetobacter* pilins is underpinned by functional differentiation.

Experimental Procedures

Protein Expression and Purification—Codon-optimized sequences of PilA from *A. baumannii* ACICU and *A. nosocomialis* M2, starting with alanine 23, were cloned into a pETM44 vector with an N-terminal His_6 tag. These clones were transformed into BL21 (DE3) pLysS cells and grown to saturation overnight with shaking at 37 °C in LB medium with 50 μg/ml ampicillin. These saturation cultures were then diluted into fresh LB-ampicillin and grown to an optical density (OD) of 0.4–0.6 at 37 °C. These flasks were transferred to a refrigerated orbital shaker and cooled to 18 °C before induction with 30 mM isopropyl β-D-1-thiogalactopyranoside. These flasks were allowed to grow overnight before being harvested by centrifugation at 7500 × *g* for 10 min. The cells were then lysed using lysozyme (0.25 mg/ml final concentration) for 10 min, and the resulting lysate was centrifuged again, this time at 20,000 × *g* for 30 min. The supernatant was purified using a nickel-nitrilotriacetic acid column, and the elution was further purified by size exclusion chromatography over a GE Healthcare S200 Superdex column using an ÅKTA Purifier FPLC.

For crystallization, MBP-PilA^{ACICU}, MBP-PilA^{BIDMC57}, and MBP-PilA^{M2} were cloned and expressed as described previously (7). Briefly, the sequences of PilA from *A. baumannii* ACICU and *A. nosocomialis* M2, starting with alanine 23, were cloned into a maltose-binding protein fusion vector, making use of surface entropy reduction mutations (pMal E) described previously (44). A C-terminal His_6 tag was included for ease of purification. These clones were transformed, expressed, and purified as described above.

Structure Determination and Refinement—All MBP fusion proteins were initially screened by sitting drop vapor diffusion at a concentration of 20 mg/ml in 20 mM Bis-Tris, pH 6.0, 50 mM maltose.

MBP-PilA^{ACICU}—MBP-PilA^{ACICU} was initially crystallized in the Hampton Research Index screen, condition D6: 0.1 M Bis-Tris, pH 5.5, 25% (w/v) polyethylene glycol 3350. These conditions were optimized to 0.1 M Bis-Tris, pH 5.5, 22.5% (w/v) polyethylene glycol 3000, 0.3 M 1,6-hexanediol, 5 mM maltotriose in place of maltose. Crystals were grown in sitting drops at room temperature and took ~48 h to grow at a protein concentration of 5 mg/ml. They were then harvested and flash cooled in the mother liquor supplemented with 20% glycerol. Data were collected at the Stanford Radiation Source, the National Light Source beam line X25 in Brookhaven, NY, and eventually the data set used to resolve the structure was collected at the Advanced Photon Source, General Medical Sciences and Cancer Institutes Structural Biology Facility, beam line 23-ID-D.

MBP-PilA^{BIDMC57}—MBP-PilA^{BIDMC57} was initially crystallized in the Molecular Dimensions Morpheus screen, condition A12: 0.1 M Bicine/Trizma (Tris base), pH 8.5, 12.5% (w/v) PEG 1000, 12.5% (w/v) PEG 3350, 12.5% (v/v) MPD, 0.03 M $CaCl_2$, 0.03 M $MgCl_2$. The optimal conditions were 0.1 M Bicine/Trizma, pH 8.0, 12.5% (w/v) PEG 1000, 12.5% (w/v) PEG 3350, 12.5% (v/v) MPD, 0.06 M $CaCl_2$, 0.06 M $MgCl_2$, 50 mM NaCl, 3% EtOH. Crystals were grown in hanging drops at room temperature and took ~72 h to grow at a protein concentration of 10 mg/ml. They were then harvested and flash cooled in the mother liquor supplemented with 20% glycerol. Data were collected at the Stanford Synchrotron Radiation Lightsource, beam line 12-2.

MBP-PilA^{M2}—MBP-PilA^{M2} was initially crystallized in the Molecular Dimensions Morpheus screen, condition A12: 0.1 M Bicine/Trizma base, pH 8.5, 12.5% (w/v) PEG 1000, 12.5% (w/v) PEG 3350, 12.5% (v/v) MPD, 0.03 M $CaCl_2$, 0.03 M $MgCl_2$. The optimal conditions were 0.1 M Bicine/Trizma, pH 8.0, 12.5% (w/v) PEG 1000, 12.5% (w/v) PEG 3350, 12.5% (v/v) MPD, 0.06 M $CaCl_2$, 0.06 M $MgCl_2$. Crystals were grown in sitting drops at room temperature and took ~72 h to grow at a protein concentration of 10 mg/ml. They were then harvested and flash cooled in the mother liquor supplemented with 20% glycerol. Data were collected at the Advanced Photon Source, GM/CA, beam line 23-ID-B.

The ACICU and M2 data sets were processed with XDS (45); the BIDMC 57 data set was processed with HKL2000 (46). Molecular replacement was carried out by Phaser (47) using a sequential search of 1) maltose-binding protein and 2) PilA from *P. aeruginosa* strain K (PAK). Phenix and Coot were used for phasing, building, and refinement (48–51). The

crystallographic parameters of the refined data are summarized in Table 1.

Differential Scanning Fluorometry—Melting curves for pilin headgroups were obtained by the addition of SYPRO Orange protein stain (Sigma-Aldrich) and thermal denaturation in an iQ5 RT-PCR cycler. The buffer conditions were 10 mM $NaPO_4$, 150 mM NaCl, 25 mM DTT. All measurements were made in triplicate. The resulting curves were normalized and fit using the Boltzmann equation to determine the melting temperature for each protein. Similar T_m values were obtained by circular dichroism (supplemental Fig. 6) (6, 52).

Pilus Modeling—Full-length $PilA^{ACICU}$ and $PilA^{M2}$ were modeled based on the structure of the full-length PAK pilin (53). The initial models of the pili were created by superimposition onto a model of the *Neisseria gonorrhoeae* type IV pilus filament (Protein Data Bank code 2HIL) (54), and the N-terminal helix position was adjusted to eliminate clashes between subunits. The resulting models were then minimized as rigid bodies using UCSF Chimera (55).

Glycan Modeling—The glycans attached to $PilA^{ACICU}$ and $PilA^{M2}$ (supplemental Fig. 2) were modeled using the PyRosetta protein structural modeling suite (56) with extensions for non-protein polymer units for the glycans (57). The initial models were generated in the Discovery Studio Visualizer (BIOVIA, Discovery Studio Modeling Environment, Release 4.5, 2015, Dassault Systèmes, San Diego, CA). Then the glycans were modeled using the FloppyTail algorithm (58) altered for use in glycans. The protocol consists of two parts. In the low resolution part, a random perturbation of the torsion angles was applied. The high resolution parts of the structures were refined by applying a smaller perturbation of the torsion angles, side-chain packing, and minimization. With this protocol, 6000 structures of $PilA^{ACICU}$ and 6000 structures of $PilA^{M2}$ were generated.

Surface Area Calculations—The 10 best scoring models were used for surface area calculations for each pilus. Exposed surface areas for pilins with and without glycans were calculated using the pilus and glycan models described above and the AreaIMol module of CCP4 (59) using a 1-nm spherical probe. C-terminal glycosylation reduces the exposed surface area from 3078 to 1801 Å ($PilA^{ACICU}$) and from 2938 to 2218 Å ($PilA^{M2}$).

Cell Adhesion—A549 human airway adenocarcinoma cells (52) (CCL 185, American Type Culture Collection (ATCC), Manassas, VA) or Detroit 562 pharyngeal carcinoma cells (53) (ATCC CCL 138) were seeded in 24-well culture plates and cultured at 37 °C in 5% CO_2 to 2.0×10^5 cells/well in Dulbecco's modified Eagle's medium containing 10% fetal bovine serum, 2.0 mM glutamine, 100 units/ml penicillin, and 100 μg/ml streptomycin. The cells were washed twice with PBS, pH 7.2; fixed for 10 min at room temperature with 2.5% (v/v) glutaraldehyde in PBS, pH 7.2; and washed three times with PBS, pH 7.2 as described (60, 61). *A. nosocomialis* M2 was cultured overnight in Luria-Bertani broth; washed twice with PBS, pH 7.2; resuspended in PBS, pH 7.2 containing 2.0 mg/ml glucose; and quantified spectrophotometrically at A_{600}. Fixed A549 or Detroit 562 cells (2.0×10^5/well) were incubated with 2.0×10^7 colony-forming units (cfu)/well *A. nosocomialis* M2 in 0.5 ml for 40 min at 37 °C and washed three times with PBS, pH 7.2. Bound bacteria were released with 0.05% trypsin, EDTA, and bound cfu were quantified on Luria-Bertani agar plates as described (60, 61). Significance was determined by Student's *t* test.

Figures—All depictions of protein structures were created using PyMOL (Schrödinger LLC) or UCSF Chimera (55). Sequence logos were created using WebLogo 3.4.

Results

Acinetobacter Species Produce Type IV Pilins with Diverse C Termini—Although all strains of *Acinetobacter* carry the genes necessary to produce type IV pili, and the majority of those genes are highly conserved, the protein sequence of the major pilin, PilA, exhibits considerable variation in the soluble domain. In addition to this variation in amino acid sequence, Harding *et al.* (38) noted that strains from multiple *Acinetobacter* species with a serine residue at the C terminus of the major pilin also expressed an *O*-OTase similar to TfpO/PilO *O*-OTase from *P. aeruginosa* in addition to the PglL-like *O*-OTase found in all *Acinetobacter* strains. Analysis of *pilA* in 49 publically available *A. baumannii* genomes, 25 with a *tfpO*-like *O*-oligosaccharyltransferase gene immediately after *pilA* and 24 without, shows considerable variation in both groups. All 25 *tfpO*+ strains also have *pilA* genes with C-terminal serine residues.

Fig. 1 shows dendrograms of PilA sequences for each of the four *Acinetobacter* species in the Acb complex. Those strains that contain a *tfpO* gene and end their PilA sequence with a serine residue are marked with an *asterisk* to indicate putative glycosylation at the C terminus. In *A. baumannii*, the majority of these strains can be divided into two large clusters. The first (highlighted in *orange*) corresponds to the international clone II group, which is responsible for 50% of hospital infections worldwide (62). The second cluster (highlighted in *blue*) contains the type strain ATCC 19606. The largest cluster of *tfpO*− strains includes the international clone I group. Importantly, representatives of these two clusters can be found in each of the other members of the Acb complex. In particular, PilA proteins from *A. baumannii* $PilA^{BIDMC57}$ and *A. nosocomialis* $PilA^{M2}$ are highlighted because their nucleotide sequences are over 99% identical.

To better understand why such diversity exists in the type IV pili of *A. baumannii*, we resolved high resolution structures of PilA proteins representative of these two major clusters. From the largest cluster, *A. baumannii* ACICU (also known as H34) is an epidemic, multidrug-resistant strain belonging to the European clone II group that was isolated in an outbreak in Rome in 2005 (63). From the other large cluster, *A. baumannii* BIDMC 57 was isolated in 2013 at Beth Israel Deaconess Medical Center (Boston, MA) and sequenced at the Broad Institute (Cambridge, MA), and *A. nosocomialis* M2 (referred to as *A. baumannii* M2 in some earlier publications) (33, 64, 65) was isolated in 1996 from a hip infection of a patient at Cleveland MetroHealth Systems (Cleveland, OH).

High Resolution Structure of $PilA^{ACICU}$—We determined the x-ray crystal structure of PilA from *A. baumannii* ACICU as a C-terminal fusion to maltose-binding protein to a resolution of 2.0 Å (Table 1). As depicted in Fig. 2, the overall fold of $PilA^{ACICU}$ is very similar (r.m.s.d. = 2.19 Å) to PilA from PAK, differ-

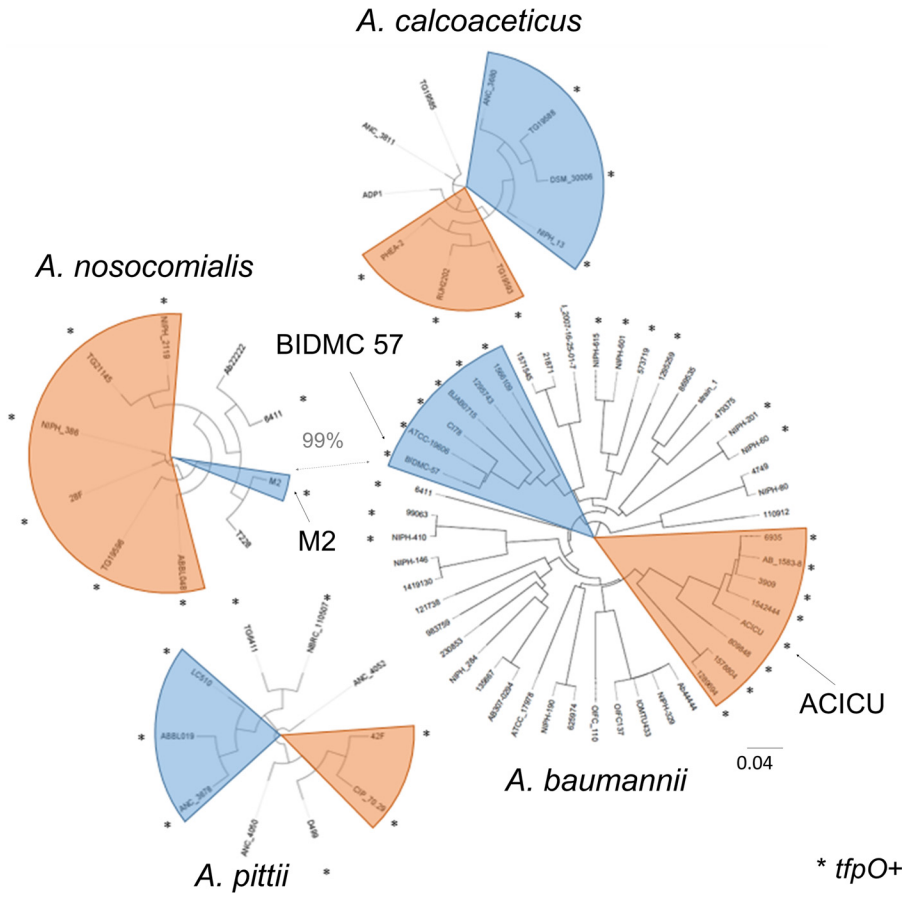

FIGURE 1. **Dendrogram of *Acinetobacter* PilA.** Dendrograms of PilA from *A. baumannii*, *A. nosocomialis*, *A. calcoaceticus*, and *A. pittii* are shown. Highlighted in *orange* are strains similar to PilA^{ACICU}, and highlighted in *blue* are those similar to PilA^{BIDMC57}. Strains with a gene homologous to *tfpO* following their *pilA* gene and a C-terminal serine in PilA are marked with an *asterisk*.

TABLE 1

Crystallographic parameters

Values in parentheses are for the highest resolution shell. r.m.s., root mean square. CC, correlation coefficient; CC1/2, Pearson correlation coefficient between half-datasets.

	MBP- PilA^{ACICU}	MBP-PilA^{BIDMC57}	MBP-PilA^{M2}
Resolution range (Å)	41.02–1.975 (2.046–1.975)	43.93–2.2 (2.279–2.2)	29.44–1.801 (1.865–1.801)
Space group	P 1 21 1	C 1 2 1	C 1 2 1
Unit cell (Å)	41.018, 128.3, 92.505, 90, 90, 90	175.07, 56.636, 49.997, 90, 91.6, 90	173.883, 55.334, 49.67, 90, 91.52, 90
Total reflections	105,740 (2,931)	125,933 (5,583)	150,644 (8,909)
Unique reflections	53,305 (1,577)	23,793 (2,036)	42,472 (3,492)
Multiplicity	2.0 (1.9)	5.3 (2.7)	3.5 (2.6)
Completeness (%)	79.68 (23.63)	94.85 (82.26)	96.82 (79.43)
Mean $I/\sigma(I)$	12.43 (2.50)	11.1 (1.70)	14.90 (1.77)
Wilson B-factor	19.31	35.78	27.29
R_{merge}	0.04968 (0.6135)	0.341 (1.10)	0.05086 (0.5152)
R_{meas}	0.07026	0.375	0.06005
CC1/2	0.992 (0.184)	0.966 (0.314)	0.998 (0.791)
CC*	0.998 (0.558)	0.991 (0.691)	1 (0.94)
R_{work}	0.1807 (0.2635)	0.2109 (0.2950)	0.1889 (0.3638)
R_{free}	0.2408 (0.3457)	0.2440 (0.3336)	0.2280 (0.3943)
r.m.s. (bonds)	0.008	0.013	0.008
r.m.s. (angles)	1.09	1.33	1.18
Ramachandran favored (%)	98	97	96
Ramachandran allowed (%)	2	2	1
Ramachandran outliers (%)	0	0.62	0.83
Clashscore	5.03	2.43	9.08
Average B-factor	26.3	28.10	37.1
Macromolecules	25.9	27.30	37
Ligands	19.7	53.10	34.1
Solvent	30.6	41.90	40.20

ing primarily in the $\alpha\beta$-loop (the loop beginning with the end of the initial α-helix and ending with the beginning of the first β-strand) (53). Among the differences between PilA from PAK and from ACICU are the α-helical character of the ACICU $\alpha\beta$-loop and the longer length of the loop between the third and fourth strands of the central β-sheet. Combined, these features give PilA^{ACICU} an axis of pseudosymmetry running diagonally across the molecule from the helix in the $\alpha\beta$-loop to the small

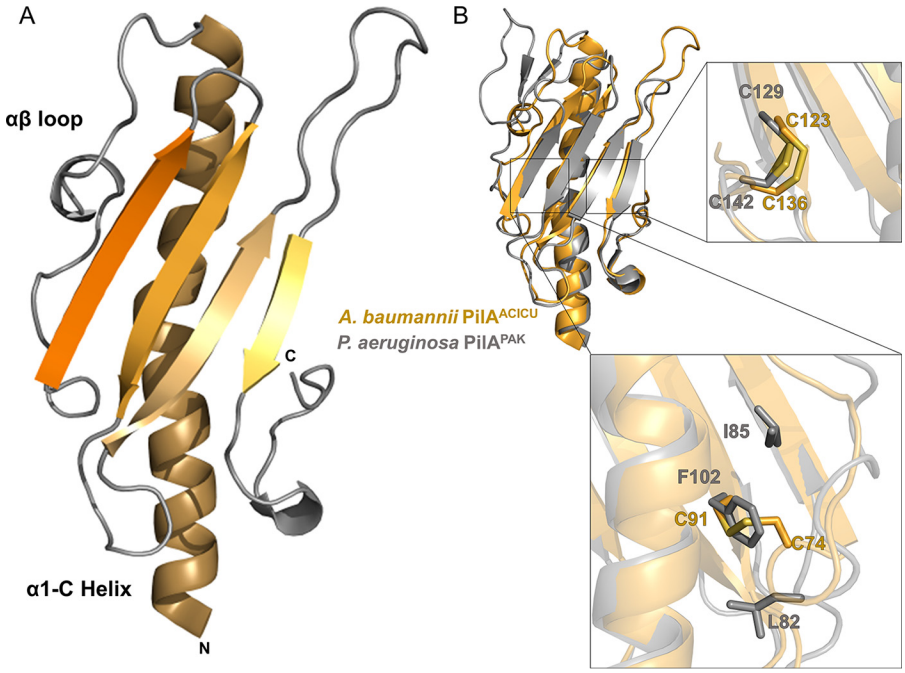

FIGURE 2. **Structure of PilA^{ACICU}.** *A*, schematic representation of PilA^{ACICU} beginning with alanine 23. *B*, superimposition of PilA^{ACICU} (*gold*) with PilA^{PAK} (*gray*); the *inset panels* show the two regions containing disulfide bonds in PilA^{ACICU}.

helical region in the C terminus, a feature also found in the structure of PilA from *P. aeruginosa* K122-4 (66). Notably, contacts between pilin headgroups in a pilus typically occur primarily between these same regions of the protein (2).

PilA^{ACICU} contains two disulfide bonds. One, between residues 123 and 136, is analogous to the C-terminal disulfide bond also found in PilA^{PAK}, which is nearly universal in type IV pili from Gram-negative bacteria. The other, between residues 74 and 91, spans the first two strands of the central β-sheet (Fig. 2*B*). However, we note that this additional disulfide bond in PilA^{ACICU} (relative to PilA^{PAK}) does not result in any substantial rearrangement of the protein backbone.

High Resolution Structures of PilA^{BIDMC57} and PilA^{M2}—Although all *Acinetobacter* PilA sequences are nearly identical in the N-terminal hydrophobic α-helix, they diverge substantially beyond that point (*e.g.* PilA^{ACICU} and PilA^{BIDMC57} are 35% identical from alanine 23 onward). However, the sequence variability of type IV pilins is such that homologs sharing only 30–40% sequence identity commonly have strikingly similar folds (the headgroups of PilA^{PAK} and PilA^{ACICU} are 30% identical in sequence). To determine whether those pilins from the type strain cluster represented a distinct fold from those from the predominant international clone II cluster, we determined the x-ray crystal structures of PilA from *A. baumannii* BIDMC 57 and *A. nosocomialis* M2 as C-terminal fusions to MBP to resolutions of 2.2 and 1.8 Å, respectively (Table 1).

Although retaining the typical type IV pilin fold, the structure of PilA^{BIDMC57} differs notably from that of PilA^{ACICU} and PilA^{PAK} with its fold showing somewhat of an inversion along the previously described axis of pseudosymmetry (Fig. 3*A*), possessing an α-helix at the C terminus rather than the N terminus. The PilA^{BIDMC57} αβ-loop contains 1) a short β-strand rather than an α-helix at its C terminus and 2) a seven-residue α-helix not found in PilA^{ACICU}. This rearrangement results in the C terminus of PilA^{BIDMC57} being shifted 13 Å relative to PilA^{ACICU} when the two pilin headgroups are superimposed (Fig. 3*D*). Although there are few prior examples of multiple high resolution structures being solved from a single species, this degree of structural variation (r.m.s.d. = 4.17 Å) is greater than is expected within a given species. All three known structures of *Clostridium difficile* PilA1 are within 1-Å r.m.s.d. of each other (7), and PilA^{PAK} and PilA^{K122-4} from *P. aeruginosa* are within 2 Å r.m.s.d. of each other and have superimposable C termini (53, 66). As expected from their sequence identity of over 99%, *A. baumannii* PilA^{BIDMC57} and *A. nosocomialis* PilA^{M2} have nearly identical structures as well, differing only in conformations of the αβ-loop and the loop between the fourth and fifth β-strands (Fig. 3*B*).

Structural Implications for PilA^{BIDMC57} and PilA^{ACICU} Assembly—Of all the component proteins of a type IV pilus system, including major and minor pilins, extension and retraction ATPases, and other pilus biogenesis machinery, the major pilin protein is always the least conserved within a given species. However, the major pilin must retain the ability to assemble into a pilus, slowing the rate of variation in regions involved in intersubunit interactions. Although in some species the sequence variability of the major pilin is confined to hypervariable regions that are solvent-exposed in the assembled pilus (14), only the hydrophobic α1-N helix is well conserved in *A. baumannii* PilA (Fig. 3*C*). To understand how surface polymorphisms in PilA might impact pilin polymerization, we created models of *A. baumannii* pilus fibers from PilA^{ACICU} and PilA^{BIDMC57} based on the *N. gonorrhoeae* pilus (54) and compared the interactions between the pilin headgroups. Despite a sequence identify of only 35% between the PilA^{ACICU} and PilA^{BIDMC57} proteins (residues 23–136), many chemical moieties can be found in similar positions (Fig. 3*D*). These relationships are not obvious from a sequence alignment of the two

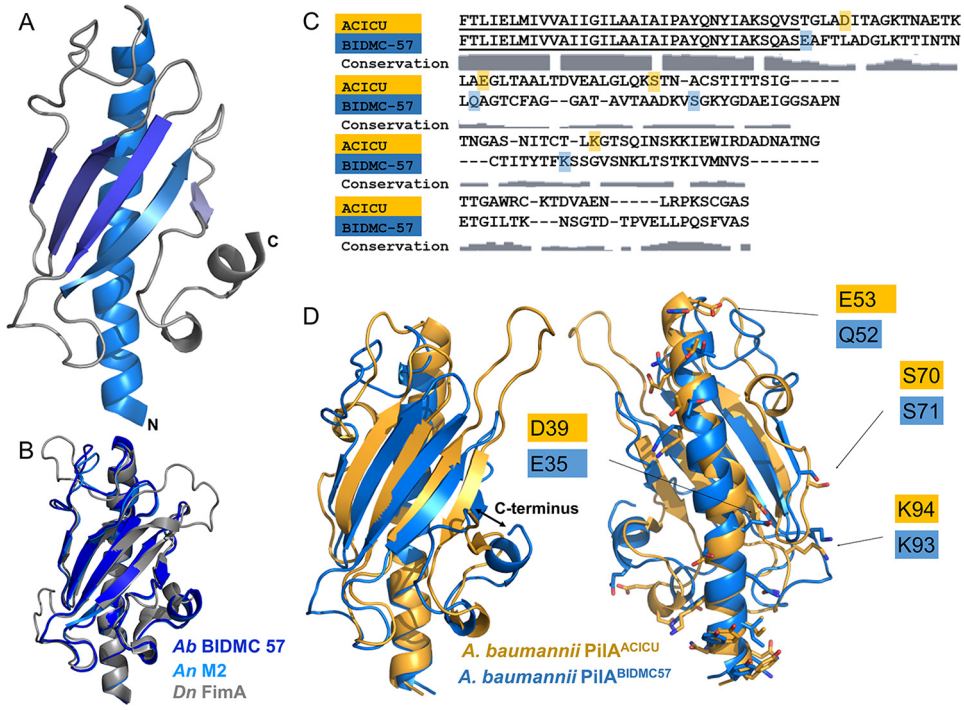

FIGURE 3. **Structure of PilA^{BIDMC57}.** *A*, schematic representation of PilA^{BIDMC57} beginning with alanine 23. *B*, superimposition of PilA^{BIDMC57} (*dark blue*) with PilA^{M2} (*light blue*) and FimA (*gray*). *C*, sequence alignment of PilA^{ACICU} and PilA^{BIDMC57}; conservation of amino acid sequence in PilA across *A. baumannii* (*Ab*) from a global alignment is indicated below. *D*, superimposition of PilA^{ACICU} (*gold*) and PilA^{BIDMC57} (*blue*).

protein sequences (Fig. 3*C*) but become clear upon superimposition of the two structures. One implication of these data is that despite their divergence in sequence the major pilins of the various *Acinetobacter* strains may be assembled through similar networks of non-covalent interactions.

Type IV Pili Promote Adhesion to A549 Cells—The resemblance of *A. baumannii* type IV pili to other type IVa pilus systems (particularly *P. aeruginosa* and *D. nodosus*) led us to hypothesize that they may have overlapping functions. Previously, *Acinetobacter* type IV pili have been shown to be essential for natural transformation and twitching motility, but few data are available about their roles in infection-associated processes such as adherence to host cells or biofilm formation. To determine whether type IV pili play a role in bacterial host-cell adhesion, we measured the ability of wild type *A. nosocomialis* M2 and mutants with altered type IV pili biogenesis phenotypes to bind to immortalized lung (A549) and nasopharyngeal (Detroit 562) epithelial cells *in vitro*. We found that the Δ*pilA* strain, which produces no type IV pili, exhibited reduced adhesion to A549 cells *in vitro* and that wild type adhesion was restored after complementation with the wild type *pilA* gene (Fig. 4). To probe the importance of C-terminal glycosylation in this process, we also tested a Δ*pilA* strain complemented with *pilA* point mutant S136A, which cannot be glycosylated. Wild type PilA and PilA(S136A) are equally capable of complementing the adhesion defect of the Δ*pilA* mutant strain, indicating that pilin glycosylation plays no significant role in host cell adhesion. Increased binding by the Δ*pilT* mutant of M2, which is known to be hyperpiliated (33, 65), shows both that increased piliation increases adhesion and that the ability to retract type IV pili is not a component of type IV pilus-mediated bacterial host-cell adhesion. We found that universally M2 binds Detroit

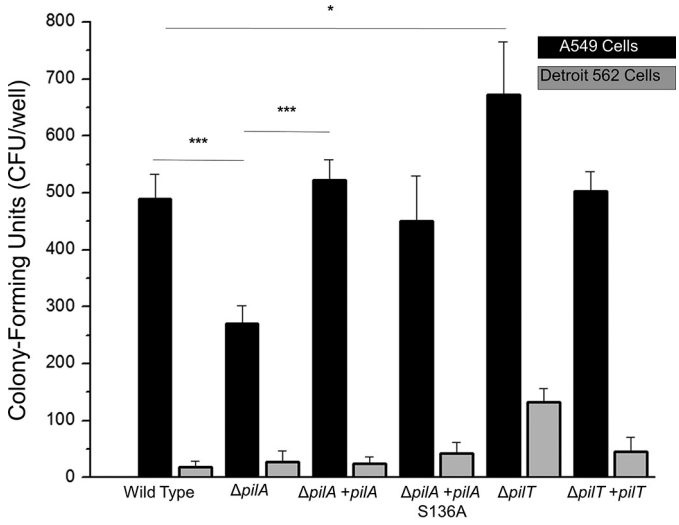

FIGURE 4. ***Acinetobacter nosocomialis* M2 adherence to host cells.** The average number of colony-forming units of *A. nosocomialis* recovered from a binding experiment with either A549 cells (*black*) or Detroit 562 cells (*gray*) is shown. Significance is marked as follows: *, $p < 0.05$; ***, $p < 0.001$. *Error bars* represent S.D.

562 cells much more weakly than A549 cells with only the Δ*pilT* strain showing any adhesion above background; this finding is similar to several strains tested by Eijkelkamp *et al.* (36). We also tested the ability of *A. nosocomialis* M2 to form a biofilm *in vitro* and found no significant difference among the wild type strain, the Δ*pilA* mutant, and the complemented mutant (supplemental Fig. 1).

C-terminal Glycans Mask the PilA Protein in Models of Pilus Assembly—There are four canonical functions for type IV pili: (i) twitching motility, (ii) horizontal gene transfer, (iii) host cell

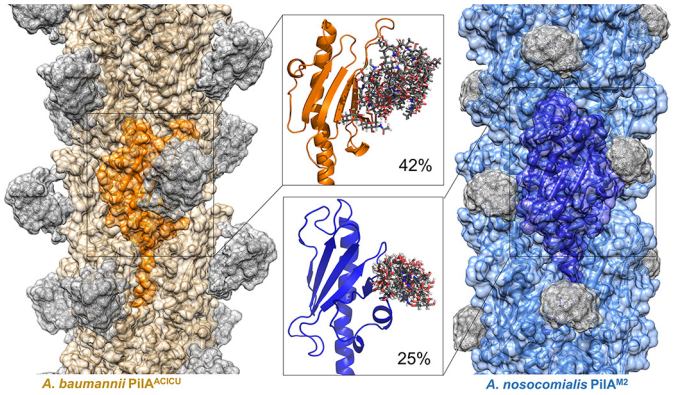

FIGURE 5. **Models of glycosylated *Acinetobacter* type IV pili.** Models of assembled type IV pili from *A. baumannii* ACICU (*orange*) and *A. nosocomialis* M2 (*blue*) are depicted with semitransparent surfaces; glycan residues are shown in *gray*. *Inset panels* show detail of the top 10 computed glycan conformations. The *percentages* note the change in surface area exposed to a 10-Å probe for each pilin monomer upon addition of the C-terminal glycan cloud.

adhesion, and (iv) bacterial self-association (biofilm formation). As described above, none of these functions are dependent on C-terminal glycosylation of the major pilin in *Acinetobacter in vitro*. However, previous studies of C-terminal glycosylation in the major pilin of *P. aeruginosa* 1244 demonstrated a significant phenotype *in vivo*. Smedley *et al.* (21) demonstrated that deletion of the *O*-oligosaccharyltransferase *tfpO* (referred to by the authors as *pilO*) reduced survival of *P. aeruginosa* 1244 in a mouse model of lung infection. More recently, the *P. aeruginosa* 1244 Δ*tfpO* mutant was found to be more vulnerable to phagocytosis mediated by opsonization (67, 68).

Because opsonization is mediated by the binding of host immune proteins (commonly antibodies), the latter studies support the notion that the purpose of C-terminal glycosylation could be to interfere with immune recognition *in vivo*. Similarly, Gault *et al.* (25) recently showed that hypervirulent *N. meningitidis* strains with class II pilins are more heavily glycosylated than their class I counterparts.

To measure the extent to which C-terminal glycosylation of PilA^{ACICU} and PilA^{M2} would mask the pilin protein from binding, we modeled the full-length pilins and pilus fibers and measured the effect of glycosylation on the accessible surface area of each protein in its native context. We modeled an ensemble of each glycan based on the repeating unit of the major polysaccharide glycan and minimized each structure using Rosetta (69). The 10 best scoring glycan conformations were then combined to approximate the native conformational ensemble.

We then measured the differences in accessible surface area using a 10-Å particle probe to approximate the surface area needed for protein binding. The resulting models are shown in Fig. 5, and the change in accessible surface area for each protein is displayed in the *inset panel*. In both cases, C-terminal glycosylation reduces the exposed surface area (by 42% for PilA^{ACICU} and by 25% for PilA^{M2}). The greater coverage of the PilA^{ACICU} protein stems from the greater flexibility of the linear PilA^{ACICU} glycan (in contrast to the branched PilA^{M2} glycan) (supplemental Fig. 2), which results in a more diverse conformational ensemble.

If C-terminal glycosylation in *Acinetobacter* type IV pili reduces recognition by host immune proteins, one might expect that the pilins from strains lacking a C-terminal glycan would face greater pressure to diversify as has been shown in *N. meningitidis* (25). Using our alignment of 49 PilA sequences, we separated protein sequences into *tfpO*− and *tfpO*+ groups and compared the variability of their surface-exposed residues. For the *tfpO*− group, we modeled the structure of PilA^{AYE} (an international clone I strain) based on the structure of PilA^{ACICU}. Supplemental Fig. 3*A* shows that, although overall the surface residue variability follows a similar pattern in the two groups, there is a region near the C terminus that is more conserved in the *tfpO*+ strains. Supplemental Fig. 3*B* shows sequence logos of this region for both groups. These data support a model in which C-terminal glycosylation in type IV pili exists, at least in part, as a countermeasure to the host humoral immune response.

Variation in Acinetobacter pilA Is Driven by Evolutionary Pressure—To understand the basis for the structural resemblance of PilA^{ACICU} and PilA^{BIDMC57} of *A. baumannii* to *P. aeruginosa* PilA^{PAK} and *D. nodosus* FimA, respectively, we compared nucleotide and amino acid sequences for the major pilin from 11 representative genomes from each of the three species (Fig. 6). To evaluate the possibility that the cross-species similarities in *pilA* arose from horizontal gene transfer, we aligned the sequences of 54 nucleotides encoding the first 18 residues of the mature protein product, which is identical (FTLIELMIVVAIIGILAA) in all 33 amino acid sequences.

Fig. 6*A* shows that, based on silent variations in these nucleotide sequences, the pilin genes can be separated neatly into three clusters based on species. That is, despite their dissimilarity in amino acid sequence, the nucleotide sequences for the α1-N domain of *pilA*^{ACICU} and *pilA*^{BIDMC57} more closely resemble each other than their equivalents from *P. aeruginosa* and *D. nodosus*. However, when mature PilA amino acid sequences are aligned, all three of the resulting clusters contain representatives from multiple sequences. As they are labeled in Fig. 6*B*, cluster I contains the majority of the *D. nodosus* FimA serotypes (including serotype A, the sequence of Protein Data Bank code 3SOK) as well as *A. baumannii* PilA^{BIDMC57} and PilA$^{ATCC\ 19606}$. Cluster II contains PilA^{ACICU} as well as *P. aeruginosa* PilA^{PAK} and PilA^{PAO1}. Cluster III consists of two FimA sequences that contain C-terminal disulfide bonds, *A. baumannii* PilA^{135867} and PilA^{121738}, and the *P. aeruginosa* PilA sequences with C-terminal serine residues.

The *A. baumannii* sequences from each of the three clusters are shown in Fig. 6*C*. Cluster II contains species from the international clone I group, whereas cluster III contains species from the international clone II group. Cysteine residues are highlighted in *yellow* and indicate differential disulfide bonding patterns between the three clusters; cluster III PilA sequences contain two disulfide bonds, and the majority of cluster I sequences do not contain a disulfide bond at the C terminus. However, all sequences in cluster I, from both *Acinetobacter* and *Dichelobacter*, contain hydrophobic residues aligned to isoleucine 106 and leucine 129 (highlighted in *violet*). These data support the hypothesis that variation in *Acinetobacter pilA* is the result of common evolutionary pressures that are common to *A. bau-*

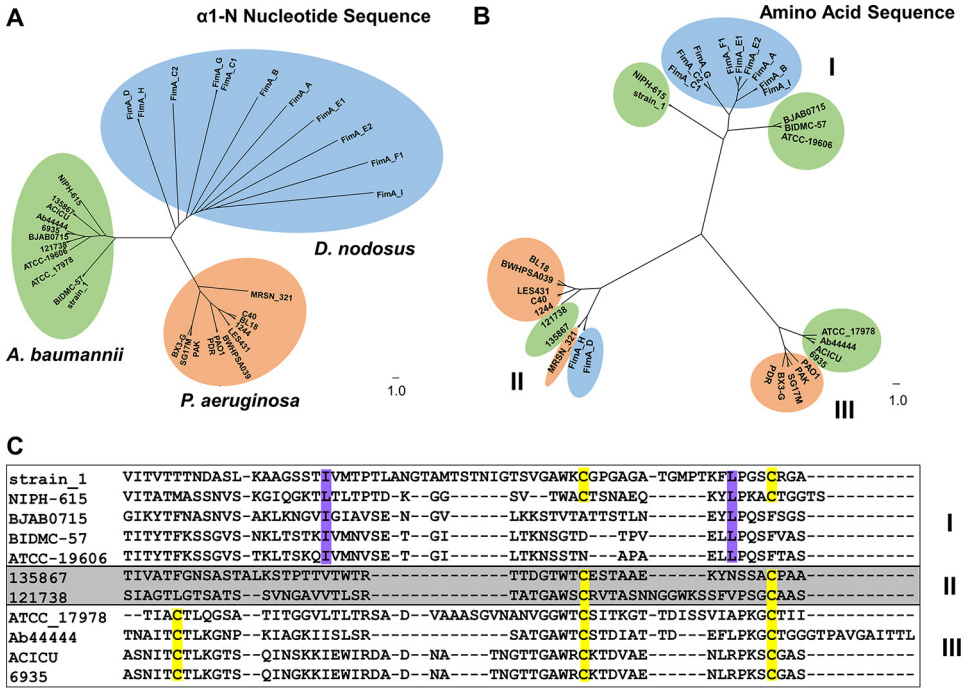

FIGURE 6. **Divergent evolution of *Acinetobacter* PilA.** *A*, dendrogram of the nucleotide sequence of the a1-N helix. Sequences from *A. baumannii* are highlighted in *green*, *D. nodosus* is in *blue*, and *P. aeruginosa* is in *orange*. *B*, dendrogram of the pilin amino acid sequence; sequences are colored identically to *A*. *C*, comparison of the three branches of *A. baumannii* PilA. Cysteine residues are highlighted in *yellow*, and the conserved C-terminal hydrophobic residues in cluster I are highlighted in *violet*.

mannii BIDMC 57 and *D. nodosus* (serotype A) and conversely *A. baumannii* ACICU and *P. aeruginosa* PAK but not to *A. baumannii* as a whole, resulting in a structural divergence of *A. baumannii* PilA.

Hydrophobic Interactions Stabilize the PilA^{M2} C Terminus—One notable aspect of the PilA^{BIDMC57} and PilA^{M2} structures is that, unlike PilA^{ACICU}, they contain only a single disulfide bond between residues 56 and 86 in the $\alpha\beta$-loop and the first strand of the β-sheet, respectively, rather than a disulfide bond at the C terminus of the pilin headgroup (Fig. 7*A*). The addition of covalent disulfide bonds is typically understood to be a mechanism of stabilization in polypeptides, and hence the C-terminal disulfide bond, which is nearly ubiquitous in type IV pilins, is thought to be conserved to stabilize the pilin fold (3).

However, the lack of a C-terminal disulfide bond is not unique to *Acinetobacter* and, in fact, was observed previously in the structure of FimA from *D. nodosus* (serotype A) that PilA^{BIDMC57} and PilA^{M2} closely resemble (Fig. 7*B*). The principal difference between the two folds is that the shorter loops of *Acinetobacter* PilA^{BIDMC57} and PilA^{M2} result in a more compact structure. The lone disulfide bond in PilA^{BIDMC57} and PilA^{M2} is found in a position identical to the disulfide bond in FimA and the N-terminal disulfide bond in PilA$^{K122\text{-}4}$ (Fig. 7*A*). As PilA^{BIDMC57}, PilA^{M2}, and FimA have such similar folds and both lack a disulfide bond at the C terminus, we compared the structures of their C termini for common structural features that might explain the absence of a C-terminal disulfide bond. Because *D. nodosus* is an obligate anaerobe and cysteine residues are more likely to be reduced in anaerobic environments, one explanation for the structural convergence of PilA^{M2} and FimA (serotype A) is that they use pilin folds, which are less reliant on a C-terminal disulfide bond for stability.

Hartung *et al.* (70) noted three non-covalent interactions in FimA that are in a similar position to the disulfide bond found in other pilins from Gram-negative bacteria: a backbone hydrogen bond between tyrosine 133 and valine 149, a hydrogen bond between the lysine 132 side chain and the backbone oxygen of lysine 150, and a van der Waals interaction between the tyrosine 133 phenyl ring and the aliphatic portion of the lysine 150 side chain. As no equivalents to these interactions can be found in the PilA^{BIDMC57} and PilA^{M2} structures, we turned our attention to potentially stabilizing interactions between pairs of aliphatic side chains. In FimA, leucine 124, leucine 140, leucine 142, and isoleucine 145 can potentially form several such pairs, and several would be superimposable with those formed by isoleucine 106, valine 126, leucine 129, and valine 134 in PilA^{M2} and PilA^{BIDMC57} (Fig. 7*B*).

As noted above, this pattern is conserved in all 14 sequences in cluster I with two of these positions, Ile-106 and Leu-129, being universally isoleucine, leucine, or valine. Conversely, although Ile-106 is conserved in PilA^{ACICU}, the other three positions are occupied by glutamate, arginine, and glycine.

To test our hypothesis that solvent exclusion from these aliphatic contacts stabilized PilA^{M2} in place of the canonical C-terminal disulfide bond, we measured the thermal stability of the PilA^{ACICU} and PilA^{M2} headgroups as well as a PilA^{M2} mutant with these four hydrophobic side chains truncated (I106A,V126A,L129A,V134A) using differential scanning fluorometry (Fig. 7*C*) (71). We found that although the wild type PilA^{M2} (T_m = 51.7 ± 0.2 °C) was less thermostable than PilA^{ACICU} (T_m = 55.7 °C ± 0.1), the hydrophobic C terminus of PilA^{M2} did contribute to the stability of the fold as evidenced by the lower melting temperature of the alanine mutant (T_m = 45.0 ± 0.5 °C).

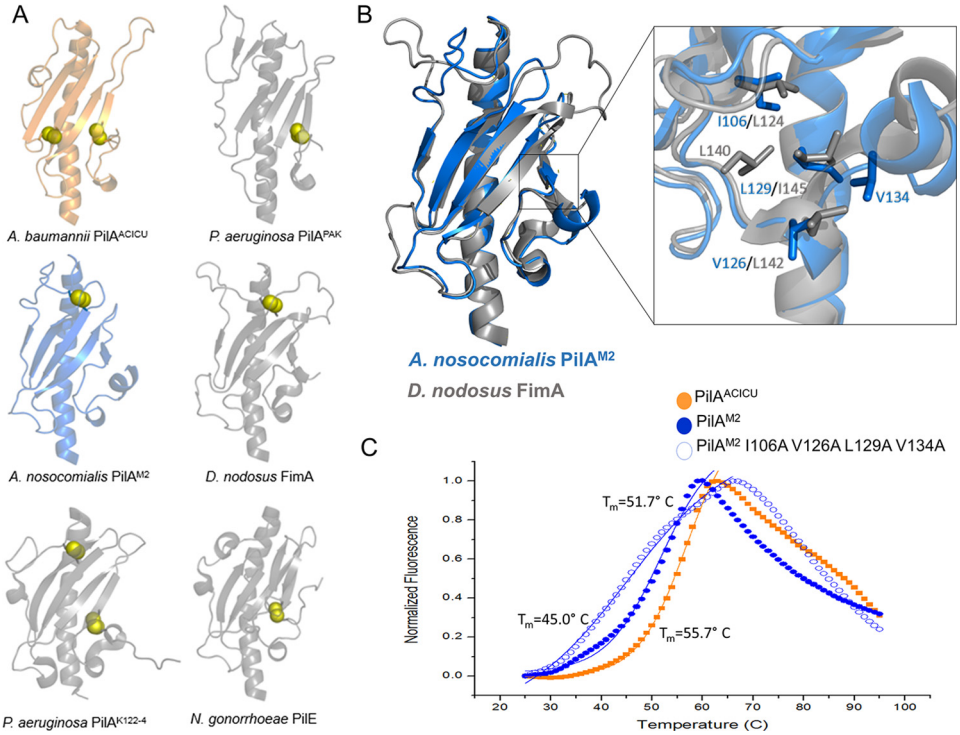

FIGURE 7. **Hydrophobic interactions in the PilA^{M2} C terminus.** *A*, schematic representations of various major pilins; disulfide bonds are marked with *yellow spheres*. *B*, superimposition of PilA^{M2} (*blue*) and FimA (*gray*); an *inset panel* shows the C-terminal region where a disulfide bond is typically found in type IV pilins. *C*, differential scanning fluorometry curves showing stability measurements for PilA^{ACICU}, PilA^{M2}, and PilA^{M2}(I106A,V126A,L129A,V134A).

Discussion

From an evolutionary standpoint, the x-ray crystal structures reported here pose three questions for us. Why have the major pilins of *A. baumannii* diverged? Why are some, but not all, PilA proteins C-terminally glycosylated? And why do the major pilins from *A. baumannii* ACICU and BIDMC 57 resemble their counterparts from other bacterial species (*P. aeruginosa* and *D. nodosus*, respectively) more closely than they do each other?

The presence of close homologs to both PilA^{ACICU} and PilA^{BIDMC57} in all four species that make up the Acb complex strongly implies that the divergence in *pilA* predates the divergence of *A. baumannii* and *A. nosocomialis*. This, combined with the similarities between PilA^{ACICU} and PilA^{PAK} and between PilA^{BIDMC57} and FimA (serotype A), suggest that the divergence in *Acinetobacter pilA* is not due to functionally neutral diversifying selection, as is thought to be the case in *Neisseria pilE*, but instead due to functionally divergent evolution.

Determining which selective pressures favor a PilA^{ACICU}/PilA^{PAK}-like structure over that of PilA^{BIDMC57} and FimA (or vice versa) is more difficult, but possibilities include altered binding specificity and stability under different environmental conditions. We note that both *Acinetobacter* and *Pseudomonas* inhabit a wide range of environments and that both genera as well as *Dichelobacter* can be isolated from soil. Differing types of soil or solid surfaces may favor one structure over another.

Another possibility is that some *Acinetobacter* type IV pilus systems are optimized for one function (horizontal gene transfer, twitching motility, or adherence) over another. Direct comparisons of twitching motility between *A. nosocomialis* M2 (cluster I) and *A. baumannii* ATCC 17978 (cluster III) do show somewhat greater motility for M2 (supplemental Fig. 4), but this complex process is impacted by many factors in addition to the sequence, structure, and function of PilA.

The related question of why *Acinetobacter pilA* genes have diverged into glycosylated and non-glycosylated forms is complicated by the fact that no functional gain or defect has been attributed to the C-terminal glycan in *Acinetobacter*, and both *tfpO*− and *tfpO*+ strains have been shown to be infectious (72, 73). Similar results were obtained for the Δ*tfpO* mutant of *P. aeruginosa* 1244, which was also found to be equally susceptible to phage attachment (21). Also arguing against a functional role for C-terminal glycans is the lack of correlation between polysaccharide and polypeptide composition; for example, PilA proteins from *A. baumannii* ATCC 19606 and *A. nosocomialis* M2 are 93% identical, but the major polysaccharide glycans from these strains are completely unrelated (supplemental Fig. 5) (38, 74). Taken together, these findings imply that even gross alterations to the exposed surface of the major pilin have little functional impact and suggest that some or all of these binding events may occur not through the major pilin but rather through the minor pilins.

It was this lack of observable phenotype that led us to search for alternative explanations for the prevalence of *tfpO*-mediated glycosylation in *Acinetobacter.* Previous work in *P. aeruginosa* 1244, demonstrating that a Δ*tfpO* mutant was more vulnerable to phagocytosis mediated by opsonization (67, 68), implied that C-terminal glycosylation formed an obstacle to binding by host immune proteins. Our quantification of the ability of *Acinetobacter* C-terminal glycans to mask their conjugate polypeptides shows that over 25% of the PilA surface area available for binding is occluded. C-terminal glycosylation

should, therefore, offer an advantage provided that the glycan surface is less vulnerable to binding by antibodies or other opsonins.

The evolutionary distance between *A. baumannii* BIDMC 57 (and *A. nosocomialis* M2) and *D. nodosus* suggests that the close resemblance between their respective pilin proteins is the result of convergent evolution. Although the functional benefit of this fold to the soil gammaproteobacteria found in class I of the alignment in Fig. 6 remains to be determined, it seems unlikely that the absence of a C-terminal disulfide bond in 12 of the 14 cluster I sequences is due to chance. We speculate that the cluster I fold may be advantageous in an anaerobic environment.

A further implication of the diversity in *Acinetobacter* type IV pilins is the challenge it poses for vaccine development. Because of their abundance in the extracellular space, type IV pili are obvious candidates for subunit vaccines and have been successfully used as such for other bacteria, including *D. nodosus* (75, 76). However, in *Acinetobacter*, the combination of variability in the PilA polypeptide with variation in polysaccharide structure in many strains may present a significant barrier to inducing a robust and durable immune response.

In conclusion, the results presented here reveal that type IV pili in *Acinetobacter* have diverged in a manner unrelated to the genetic divergence of species within the Acb complex and that similarities in type IV pili cross species, genus, and family lines. These data reinforce the principle that functional requirements determine protein structure while allowing considerable variation in sequence. These data also imply that three distinct functional classes of type IV pili exist in *Acinetobacter* and other soil gammaproteobacteria.

Author Contributions—K. H. P. conducted most of the experiments, analyzed the results, and wrote the paper. E. L. conducted the cell binding measurements. C. M. H. created the mutant *Acinetobacter* strains used in this study (with the aid of R. S. M.) and provided valuable experimental input and commentary during writing. J. W. L. and X. Z. performed the glycan conformational simulations. C. A. R. conducted the *in vitro* biofilm formation experiments. S. E. G., M. F. F., J. J. G., and E. J. S. helped to coordinate the study and write the paper.

Acknowledgments—We thank the staff at Argonne National Laboratory Advanced Photon Source, General Medical Sciences and Cancer Institutes Structural Biology Facility, beam lines 23ID-D and 23ID-B, and the staff at Stanford Synchrotron Radiation Lightsource, beam line 12-2, for technical assistance with x-ray data collection. We also thank Dr. Angela Wilks for the use of the circular dichroism spectrophotometer.

References

1. Strom, M. S., and Lory, S. (1993) Structure-function and biogenesis of the type IV pili. *Annu. Rev. Microbiol.* **47,** 565–596
2. Giltner, C. L., Nguyen, Y., and Burrows, L. L. (2012) Type IV pilin proteins: versatile molecular modules. *Microbiol. Mol. Biol. Rev.* **76,** 740–772
3. Craig, L., Pique, M. E., and Tainer, J. A. (2004) Type IV pilus structure and bacterial pathogenicity. *Nat. Rev. Microbiol.* **2,** 363–378
4. Stone, B. J., and Abu Kwaik, Y. (1998) Expression of multiple pili by Legionella pneumophila: identification and characterization of a type IV pilin gene and its role in adherence to mammalian and protozoan cells. *Infect. Immun.* **66,** 1768–1775
5. Taniguchi, T., Fujino, Y., Yamamoto, K., Miwatani, T., and Honda, T. (1995) Sequencing of the gene encoding the major pilin of pilus colonization factor antigen III (CFA/III) of human enterotoxigenic *Escherichia coli* and evidence that CFA/III is related to type IV pili. *Infect. Immun.* **63,** 724–728
6. Piepenbrink, K. H., Maldarelli, G. A., de la Peña, C. F., Mulvey, G. L., Snyder, G. A., De Masi, L., von Rosenvinge, E. C., Günther, S., Armstrong, G. D., Donnenberg, M. S., and Sundberg, E. J. (2014) Structure of *Clostridium difficile* PilJ exhibits unprecedented divergence from known type IV pilins. *J. Biol. Chem.* **289,** 4334–4345
7. Piepenbrink, K. H., Maldarelli, G. A., Martinez de la Peña, C. F., Dingle, T. C., Mulvey, G. L., Lee, A., von Rosenvinge, E., Armstrong, G. D., Donnenberg, M. S., and Sundberg, E. J. (2015) Structural and evolutionary analyses show unique stabilization strategies in the type IV pili of *Clostridium difficile*. *Structure* **23,** 385–396
8. Melville, S., and Craig, L. (2013) Type IV pili in Gram-positive bacteria. *Microbiol. Mol. Biol. Rev.* **77,** 323–341
9. Lassak, K., Ghosh, A., and Albers, S. V. (2012) Diversity, assembly and regulation of archaeal type IV pili-like and non-type-IV pili-like surface structures. *Res. Microbiol.* **163,** 630–644
10. Wall, D., and Kaiser, D. (1999) Type IV pili and cell motility. *Mol. Microbiol.* **32,** 1–10
11. Seifert, H. S., Ajioka, R. S., Marchal, C., Sparling, P. F., and So, M. (1988) DNA transformation leads to pilin antigenic variation in *Neisseria gonorrhoeae*. *Nature* **336,** 392–395
12. Takahashi, H., Yanagisawa, T., Kim, K. S., Yokoyama, S., and Ohnishi, M. (2012) Meningococcal PilV potentiates *Neisseria meningitidis* type IV pilus-mediated internalization into human endothelial and epithelial cells. *Infect. Immun.* **80,** 4154–4166
13. Bieber, D., Ramer, S. W., Wu, C. Y., Murray, W. J., Tobe, T., Fernandez, R., and Schoolnik, G. K. (1998) Type IV pili, transient bacterial aggregates, and virulence of enteropathogenic *Escherichia coli*. *Science* **280,** 2114–2118
14. Cehovin, A., Winterbotham, M., Lucidarme, J., Borrow, R., Tang, C. M., Exley, R. M., and Pelicic, V. (2010) Sequence conservation of pilus subunits in *Neisseria meningitidis*. *Vaccine* **28,** 4817–4826
15. Criss, A. K., Kline, K. A., and Seifert, H. S. (2005) The frequency and rate of pilin antigenic variation in *Neisseria gonorrhoeae*. *Mol. Microbiol.* **58,** 510–519
16. Toma, C., Kuroki, H., Nakasone, N., Ehara, M., and Iwanaga, M. (2002) Minor pilin subunits are conserved in *Vibrio cholerae* type IV pili. *FEMS Immunol. Med. Microbiol.* **33,** 35–40
17. Blank, T. E., Zhong, H., Bell, A. L., Whittam, T. S., and Donnenberg, M. S. (2000) Molecular variation among type IV pilin (*bfpA*) genes from diverse enteropathogenic *Escherichia coli* strains. *Infect. Immun.* **68,** 7028–7038
18. Maldarelli, G. A., De Masi, L., von Rosenvinge, E. C., Carter, M., and Donnenberg, M. S. (2014) Identification, immunogenicity, and cross-reactivity of type IV pilin and pilin-like proteins from *Clostridium difficile*. *Pathog. Dis.* **71,** 302–314
19. Aagesen, A. M., and Häse, C. C. (2012) Sequence analyses of type IV pili from *Vibrio cholerae*, *Vibrio parahaemolyticus*, and *Vibrio vulnificus*. *Microb. Ecol.* **64,** 509–524
20. Allison, T. M., Conrad, S., and Castric, P. (2015) The group I pilin glycan affects type IVa pilus hydrophobicity and twitching motility in *Pseudomonas aeruginosa* 1244. *Microbiology* **161,** 1780–1789
21. Smedley, J. G., 3rd, Jewell, E., Roguskie, J., Horzempa, J., Syboldt, A., Stolz, D. B., and Castric, P. (2005) Influence of pilin glycosylation on *Pseudomonas aeruginosa* 1244 pilus function. *Infect. Immun.* **73,** 7922–7931
22. Voisin, S., Kus, J. V., Houliston, S., St-Michael, F., Watson, D., Cvitkovitch, D. G., Kelly, J., Brisson, J. R., and Burrows, L. L. (2007) Glycosylation of *Pseudomonas aeruginosa* strain Pa5196 type IV pilins with *Mycobacterium*-like α-1,5-linked D-Ara*f* oligosaccharides. *J. Bacteriol.* **189,** 151–159
23. Aas, F. E., Vik, A., Vedde, J., Koomey, M., and Egge-Jacobsen, W. (2007) *Neisseria gonorrhoeae* O-linked pilin glycosylation: functional analyses define both the biosynthetic pathway and glycan structure. *Mol. Microbiol.* **65,** 607–624

24. Power, P. M., Seib, K. L., and Jennings, M. P. (2006) Pilin glycosylation in *Neisseria meningitidis* occurs by a similar pathway to wzy-dependent O-antigen biosynthesis in *Escherichia coli*. *Biochem. Biophys. Res. Commun.* **347,** 904–908
25. Gault, J., Ferber, M., Machata, S., Imhaus, A. F., Malosse, C., Charles-Orszag, A., Millien, C., Bouvier, G., Bardiaux, B., Péhau-Arnaudet, G., Klinge, K., Podglajen, I., Ploy, M. C., Seifert, H. S., Nilges, M., *et al.* (2015) *Neisseria meningitidis* type IV pili composed of sequence invariable pilins are masked by multisite glycosylation. *PLoS Pathog.* **11,** e1005162
26. Falagas, M. E., and Kopterides, P. (2006) Risk factors for the isolation of multi-drug-resistant *Acinetobacter baumannii* and *Pseudomonas aeruginosa*: a systematic review of the literature. *J. Hosp. Infect.* **64,** 7–15
27. Peleg, A. Y., Seifert, H., and Paterson, D. L. (2008) *Acinetobacter baumannii*: emergence of a successful pathogen. *Clin. Microbiol. Rev.* **21,** 538–582
28. Dijkshoorn, L., Nemec, A., and Seifert, H. (2007) An increasing threat in hospitals: multidrug-resistant *Acinetobacter baumannii*. *Nat. Rev. Microbiol.* **5,** 939–951
29. Jones, A., Morgan, D., Walsh, A., Turton, J., Livermore, D., Pitt, T., Green, A., Gill, M., and Mortiboy, D. (2006) Importation of multidrug-resistant *Acinetobacter* spp infections with casualties from Iraq. *Lancet Infect. Dis.* **6,** 317–318
30. Harding, C. M., Kinsella, R. L., Palmer, L. D., Skaar, E. P., and Feldman, M. F. (2016) Medically relevant *Acinetobacter* species require a type II secretion system and specific membrane-associated chaperones for the export of multiple substrates and full virulence. *PLoS Pathog.* **12,** e1005391
31. Chang, H. C., Wei, Y. F., Dijkshoorn, L., Vaneechoutte, M., Tang, C. T., and Chang, T. C. (2005) Species-level identification of isolates of the *Acinetobacter calcoaceticus-Acinetobacter baumannii* complex by sequence analysis of the 16S-23S rRNA gene spacer region. *J. Clin. Microbiol.* **43,** 1632–1639
32. Antunes, L. C., Visca, P., and Towner, K. J. (2014) *Acinetobacter baumannii*: evolution of a global pathogen. *Pathog. Dis.* **71,** 292–301
33. Harding, C. M., Tracy, E. N., Carruthers, M. D., Rather, P. N., Actis, L. A., and Munson, R. S., Jr.(2013) *Acinetobacter baumannii* strain M2 produces type IV pili which play a role in natural transformation and twitching motility but not surface-associated motility. *MBio* **4,** e00360-13
34. Wilharm, G., Piesker, J., Laue, M., and Skiebe, E. (2013) DNA uptake by the nosocomial pathogen *Acinetobacter baumannii* occurs during movement along wet surfaces. *J. Bacteriol.* **195,** 4146–4153
35. Nait Chabane, Y., Mlouka, M. B., Alexandre, S., Nicol, M., Marti, S., Pestel-Caron, M., Vila, J., Jouenne, T., and Dé, E. (2014) Virstatin inhibits biofilm formation and motility of *Acinetobacter baumannii*. *BMC Microbiol.* **14,** 62
36. Eijkelkamp, B. A., Stroeher, U. H., Hassan, K. A., Papadimitrious, M. S., Paulsen, I. T., and Brown, M. H. (2011) Adherence and motility characteristics of clinical *Acinetobacter baumannii* isolates. *FEMS Microbiol. Lett.* **323,** 44–51
37. Oh, M. H., and Choi, C. H. (2015) Role of LuxIR homologue AnoIR in *Acinetobacter nosocomialis* and the effect of virstatin on the expression of *anoR* gene. *J. Microbiol. Biotechnol.* **25,** 1390–1400
38. Harding, C. M., Nasr, M. A., Kinsella, R. L., Scott, N. E., Foster, L. J., Weber, B. S., Fiester, S. E., Actis, L. A., Tracy, E. N., Munson, R. S., Jr, and Feldman, M. F. (2015) *Acinetobacter* strains carry two functional oligosaccharyltransferases, one devoted exclusively to type IV pilin, and the other one dedicated to O-glycosylation of multiple proteins. *Mol. Microbiol.* **96,** 1023–1041
39. Hu, D., Liu, B., Dijkshoorn, L., Wang, L., and Reeves, P. R. (2013) Diversity in the major polysaccharide antigen of *Acinetobacter baumannii* assessed by DNA sequencing, and development of a molecular serotyping scheme. *PLoS One* **8,** e70329
40. Iwashkiw, J. A., Seper, A., Weber, B. S., Scott, N. E., Vinogradov, E., Stratilo, C., Reiz, B., Cordwell, S. J., Whittal, R., Schild, S., and Feldman, M. F. (2012) Identification of a general O-linked protein glycosylation system in *Acinetobacter baumannii* and its role in virulence and biofilm formation. *PLoS Pathog.* **8,** e1002758
41. Lees-Miller, R. G., Iwashkiw, J. A., Scott, N. E., Seper, A., Vinogradov, E., Schild, S., and Feldman, M. F. (2013) A common pathway for O-linked protein-glycosylation and synthesis of capsule in *Acinetobacter baumannii*. *Mol. Microbiol.* **89,** 816–830
42. Cagatay, T. I., and Hickford, J. G. (2008) Glycosylation of type-IV fimbriae of *Dichelobacter nodosus*. *Vet. Microbiol.* **126,** 160–167
43. DiGiandomenico, A., Matewish, M. J., Bisaillon, A., Stehle, J. R., Lam, J. S., and Castric, P. (2002) Glycosylation of *Pseudomonas aeruginosa* 1244 pilin: glycan substrate specificity. *Mol. Microbiol.* **46,** 519–530
44. Moon, A. F., Mueller, G. A., Zhong, X., and Pedersen, L. C. (2010) A synergistic approach to protein crystallization: combination of a fixed-arm carrier with surface entropy reduction. *Protein Sci.* **19,** 901–913
45. Kabsch, W. (2010) XDS. *Acta Crystallogr. D Biol. Crystallogr.* **66,** 125–132
46. Otwinowski, Z., and Minor, W. (1997) Processing of x-ray diffraction data collected in oscillation mode. *Methods Enzymol.* **276,** 307–326
47. McCoy, A. J., Grosse-Kunstleve, R. W., Adams, P. D., Winn, M. D., Storoni, L. C., and Read, R. J. (2007) Phaser crystallographic software. *J. Appl. Crystallogr.* **40,** 658–674
48. Adams, P. D., Afonine, P. V., Bunkóczi, G., Chen, V. B., Davis, I. W., Echols, N., Headd, J. J., Hung, L. W., Kapral, G. J., Grosse-Kunstleve, R. W., McCoy, A. J., Moriarty, N. W., Oeffner, R., Read, R. J., Richardson, D. C., *et al.* (2010) PHENIX: a comprehensive Python-based system for macromolecular structure solution. *Acta Crystallogr. D Biol. Crystallogr.* **66,** 213–221
49. Adams, P. D., Afonine, P. V., Bunkóczi, G., Chen, V. B., Echols, N., Headd, J. J., Hung, L. W., Jain, S., Kapral, G. J., Grosse Kunstleve, R. W., McCoy, A. J., Moriarty, N. W., Oeffner, R. D., Read, R. J., Richardson, D. C., *et al.* (2011) The Phenix software for automated determination of macromolecular structures. *Methods* **55,** 94–106
50. Adams, P. D., Grosse-Kunstleve, R. W., Hung, L. W., Ioerger, T. R., McCoy, A. J., Moriarty, N. W., Read, R. J., Sacchettini, J. C., Sauter, N. K., and Terwilliger, T. C. (2002) PHENIX: building new software for automated crystallographic structure determination. *Acta Crystallogr. D Biol. Crystallogr.* **58,** 1948–1954
51. Emsley, P., and Cowtan, K. (2004) Coot: model-building tools for molecular graphics. *Acta Crystallogr. D Biol. Crystallogr.* **60,** 2126–2132
52. Borbulevych, O. Y., Piepenbrink, K. H., and Baker, B. M. (2011) Conformational melding permits a conserved binding geometry in TCR recognition of foreign and self molecular mimics. *J. Immunol.* **186,** 2950–2958
53. Craig, L., Taylor, R. K., Pique, M. E., Adair, B. D., Arvai, A. S., Singh, M., Lloyd, S. J., Shin, D. S., Getzoff, E. D., Yeager, M., Forest, K. T., and Tainer, J. A. (2003) Type IV pilin structure and assembly: x-ray and EM analyses of *Vibrio cholerae* toxin-coregulated pilus and *Pseudomonas aeruginosa* PAK pilin. *Mol. Cell* **11,** 1139–1150
54. Craig, L., Volkmann, N., Arvai, A. S., Pique, M. E., Yeager, M., Egelman, E. H., and Tainer, J. A. (2006) Type IV pilus structure by cryo-electron microscopy and crystallography: implications for pilus assembly and functions. *Mol. Cell* **23,** 651–662
55. Pettersen, E. F., Goddard, T. D., Huang, C. C., Couch, G. S., Greenblatt, D. M., Meng, E. C., and Ferrin, T. E. (2004) UCSF Chimera—a visualization system for exploratory research and analysis. *J. Comput. Chem.* **25,** 1605–1612
56. Chaudhury, S., Lyskov, S., and Gray, J. J. (2010) PyRosetta: a script-based interface for implementing molecular modeling algorithms using Rosetta. *Bioinformatics* **26,** 689–691
57. Drew, K., Renfrew, P. D., Craven, T. W., Butterfoss, G. L., Chou, F. C., Lyskov, S., Bullock, B. N., Watkins, A., Labonte, J. W., Pacella, M., Kilambi, K. P., Leaver-Fay, A., Kuhlman, B., Gray, J. J., Bradley, P., *et al.* (2013) Adding diverse noncanonical backbones to Rosetta: enabling peptidomimetic design. *PLoS One* **8,** e67051
58. Kleiger, G., Saha, A., Lewis, S., Kuhlman, B., and Deshaies, R. J. (2009) Rapid E2-E3 assembly and disassembly enable processive ubiquitylation of cullin-RING ubiquitin ligase substrates. *Cell* **139,** 957–968
59. (1994) The CCP4 suite: programs for protein crystallography. *Acta Crystallogr. D Biol. Crystallogr.* **50,** 760–763
60. Lillehoj, E. P., Hyun, S. W., Feng, C., Zhang, L., Liu, A., Guang, W., Nguyen, C., Luzina, I. G., Atamas, S. P., Passaniti, A., Twaddell, W. S., Puché, A. C., Wang, L. X., Cross, A. S., and Goldblum, S. E. (2012) NEU1 sialidase expressed in human airway epithelia regulates epidermal growth factor receptor (EGFR) and MUC1 protein signaling. *J. Biol. Chem.* **287,** 8214–8231

61. Lillehoj, E. P., Hyun, S. W., Liu, A., Guang, W., Verceles, A. C., Luzina, I. G., Atamas, S. P., Kim, K. C., and Goldblum, S. E. (2015) NEU1 sialidase regulates membrane-tethered mucin (MUC1) ectodomain adhesiveness for *Pseudomonas aeruginosa* and decoy receptor release. *J. Biol. Chem.* **290,** 18316–18331
62. Doi, Y., Murray, G. L., and Peleg, A. Y. (2015) *Acinetobacter baumannii*: evolution of antimicrobial resistance-treatment options. *Semin. Respir. Crit. Care Med.* **36,** 85–98
63. Iacono, M., Villa, L., Fortini, D., Bordoni, R., Imperi, F., Bonnal, R. J., Sicheritz-Ponten, T., De Bellis, G., Visca, P., Cassone, A., and Carattoli, A. (2008) Whole-genome pyrosequencing of an epidemic multidrug-resistant *Acinetobacter baumannii* strain belonging to the European clone II group. *Antimicrob. Agents Chemother.* **52,** 2616–2625
64. Carruthers, M. D., Harding, C. M., Baker, B. D., Bonomo, R. A., Hujer, K. M., Rather, P. N., and Munson, R. S., Jr. (2013) Draft genome sequence of the clinical isolate *Acinetobacter nosocomialis* strain M2. *Genome Announc.* **1,** e00906–13
65. Clemmer, K. M., Bonomo, R. A., and Rather, P. N. (2011) Genetic analysis of surface motility in *Acinetobacter baumannii*. *Microbiology* **157,** 2534–2544
66. Audette, G. F., Irvin, R. T., and Hazes, B. (2004) Crystallographic analysis of the *Pseudomonas aeruginosa* strain K122-4 monomeric pilin reveals a conserved receptor-binding architecture. *Biochemistry* **43,** 11427–11435
67. Tan, R. M., Kuang, Z., Hao, Y., and Lau, G. W. (2014) Type IV pilus of *Pseudomonas aeruginosa* confers resistance to antimicrobial activities of the pulmonary surfactant protein-A. *J. Innate Immun.* **6,** 227–239
68. Tan, R. M., Kuang, Z., Hao, Y., Lee, F., Lee, T., Lee, R. J., and Lau, G. W. (2015) Type IV pilus glycosylation mediates resistance of *Pseudomonas aeruginosa* to opsonic activities of the pulmonary surfactant protein A. *Infect. Immun.* **83,** 1339–1346
69. Simons, K. T., Kooperberg, C., Huang, E., and Baker, D. (1997) Assembly of protein tertiary structures from fragments with similar local sequences using simulated annealing and Bayesian scoring functions. *J. Mol. Biol.* **268,** 209–225
70. Hartung, S., Arvai, A. S., Wood, T., Kolappan, S., Shin, D. S., Craig, L., and Tainer, J. A. (2011) Ultrahigh resolution and full-length pilin structures with insights for filament assembly, pathogenic functions, and vaccine potential. *J. Biol. Chem.* **286,** 44254–44265
71. Huynh, K., and Partch, C. L. (2015) Analysis of protein stability and ligand interactions by thermal shift assay. *Curr. Protoc. Protein Sci.* **79,** 28.9.1–28.9.14
72. Jacobs, A. C., Thompson, M. G., Black, C. C., Kessler, J. L., Clark, L. P., McQueary, C. N., Gancz, H. Y., Corey, B. W., Moon, J. K., Si, Y., Owen, M. T., Hallock, J. D., Kwak, Y. I., Summers, A., Li, C. Z., *et al.* (2014) AB5075, a highly virulent isolate of *Acinetobacter baumannii*, as a model strain for the evaluation of pathogenesis and antimicrobial treatments. *MBio* **5,** e01076–14
73. Jones, C. L., Clancy, M., Honnold, C., Singh, S., Snesrud, E., Onmus-Leone, F., McGann, P., Ong, A. C., Kwak, Y., Waterman, P., Zurawski, D. V., Clifford, R. J., and Lesho, E. (2015) Fatal outbreak of an emerging clone of extensively drug-resistant *Acinetobacter baumannii* with enhanced virulence. *Clin. Infect. Dis.* **61,** 145–154
74. Scott, N. E., Kinsella, R. L., Edwards, A. V., Larsen, M. R., Dutta, S., Saba, J., Foster, L. J., and Feldman, M. F. (2014) Diversity within the *O*-linked protein glycosylation systems of *Acinetobacter* species. *Mol. Cell. Proteomics* **13,** 2354–2370
75. Bhardwaj, V., Dhungyel, O., de Silva, K., and Whittington, R. J. (2014) Investigation of immunity in sheep following footrot infection and vaccination. *Vaccine* **32,** 6979–6985
76. Korpi, F., Irajian, G., Mahadavi, M., Motamedifar, M., Mousavi, M., Laghaei, P., Raei, N., and Behrouz, B. (2015) Active immunization with recombinant PilA protein protects against *Pseudomonas aeruginosa* infection in a mouse burn wound model. *J. Microbiol. Biotechnol.* 10.4014/jmb.1507.07044

Structural Diversity in the Type IV Pili of Multidrug-resistant *Acinetobacter*

Kurt H. Piepenbrink, Erik Lillehoj, Christian M. Harding, Jason W. Labonte, Xiaotong Zuo, Chelsea A. Rapp, Robert S. Munson, Jr., Simeon E. Goldblum, Mario F. Feldman, Jeffrey J. Gray and Eric J. Sundberg

J. Biol. Chem. 2016, 291:22924-22935.
doi: 10.1074/jbc.M116.751099 originally published online September 15, 2016